International Journal of Mechanical and Industrial Technology ISSN 2348-7593 (Online)
Vol. 10, Issue 2, pp: (30-43), Month: October 2022 - March 2023, Available at: www.researchpublish.com

MHD Darcy-Forchheimer Slip Flow in a Porous Medium with Variable Thermo-Physical Properties

[1,2]A.L. Panya, [2]O. A. Akinyemi, [2, 3]A.M. Okedoye

[1]Department of Mathematics, College of Education, Warri, Delta State, Nigeria

[2]Department of Mathematics, Federal University of Petroleum Resources, Effurun, Delta State, Nigeria

[3]Department of Mathematics, Covenant University, Canaan Land, Ota, Ogun State, Nigeria

DOI: https://doi.org/10.5281/zenodo.7646344

Published Date: 16-February-2023

Abstract: **MHD Darcy-Forchheimer Slip Flow in a Porous Medium with Variable Thermo-Physical Properties was studied. The governing partial differential equations are converted into nonlinear ordinary differential equations using a similarity transformation and solved numerically. The variable and thermal conductivity were studied. Different physical parameters' effects on temperature, velocity and concentration distribution are studied. The effects of Darcy-Forchheimer parameter, suction/blowing parameter, velocity slip and thermal slip parameter on the velocity, temperature and mass transfer rates nature are examined with the aid of graphs. Schmidt number and Soret number effect are also presented. The results shows that when the porosity parameter is increased, the velocity of the fluid decrease, while temperature profile and skin friction decreases. Also increasing the velocity slip parameter result in increase in velocity and Nusselt number whereas the concentration decreases in same case. Also the temperature at a point decreases with increase in thermal slip parameter while the skin friction decrease in both cases.**

Keywords: **Darcy-Forchheimer, Porous medium, Slip flow, Magneto-hydrodynamics (MHD), variable viscosity, thermal conductivity.**

I. INTRODUCTION

The flow in porous medium is a well-known issue that spawned its own academic's discipline. The concept is used in a wide range of fields, including applied sciences, petroleum and construction engineering, geosciences, biology and material sciences. Slip flow in porous medium and its heat transfer taking account of its thermo-physical properties has a significant commitment to current innovations and advanced applications. Menni et al [1] report that these problems occur in barely all aspect of technological development to mention but a few, the storage of radioactive nuclear waste, separation process, filtration and transport mechanisms in aquifers, ground water pollution, geo-thermal extraction and insulation of fibre. The flow through porous media is reported extensively by the following literature review by the studies [2-4].

When a viscous fluid flows along a fixed impermeable wall, or past the rigid surface of an immersed body, an essential condition is that of the velocity at the walls or the heat or mass transfer rate at the surface. The extent to which this condition modifies the general character of the flow depends upon the thermo-physical properties like viscosity. The understanding of the thermophysical properties of some parameters associated with the fluid flows have influences on many industrial processes. In view of this, scientist has being showing high interest on the seemly behavior of fluids with thermophysical properties and subsequently studies has been done on it using the different analytical approaches which are available in many articles including Chen, C.H.[23], Elbashbeshy, E.M [24] and Elbashbeshy, E.M et al [25]. In most of the studies of this nature, some thermophysical properties of the fluid were assumed to be constant. However, it is known that these physical properties can change significantly with temperature and when their effects are taken in to consideration, the flow

characteristics are significantly changed compared to constant property case. Balla et al [5] studied the effects of variable viscosity and thermal conductivity on MHD flow of Nanofluid with thermal radiation whereby they used the weighted residual finite element method to solve the systems of equations. Chiam [6] looked at the effect of variable thermal conductivity with temperature dependent heat source/sink. Variable viscosity, chemical reaction, heat and mass transfer effect on laminar flow along a semi-infinite horizontal plate has been analyzed by Ghaly and Seddeek [7]. Odda and Farhan [8] in his work varied the fluid viscosity and the thermal conductivity as inverse linear functions of temperature on a stretching sheet and studied the effect. Seddeek and Salama [9] investigate the effect of variable viscosity and thermal conductivity taking into account the effect of a magnetic field in the presence of variable suction in an unsteady two-dimensional laminar flow of viscous incompressible conducting fluid past a semi-infinite vertical porous moving plate. Lai and Kulacki [10] examined variable viscosity effects on boundary layer flow with convective heat and mass transfer in

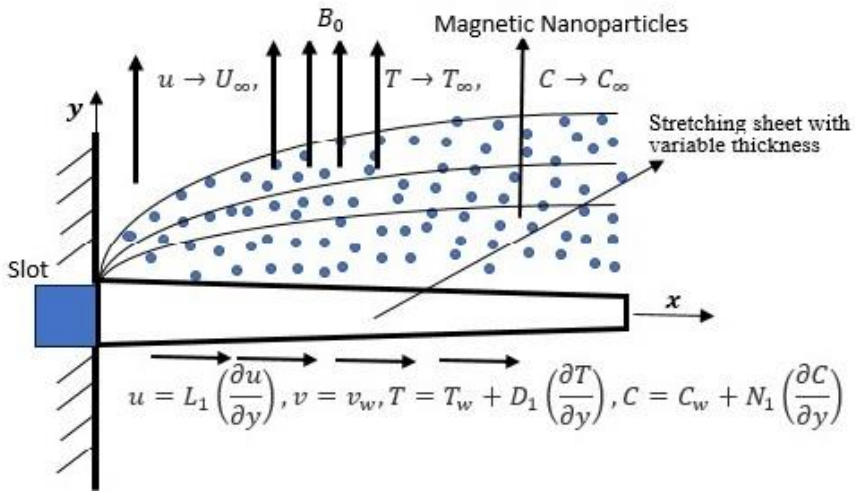

Figure 1: Flow geometry

saturated porous media. Variable viscosity and thermal conductivity effects on MHD flow and heat transfer was studied by Manjunatha and Gireesha [11]. The field of MHD was initiated by Hannes Alfven [12], for which he received the Nobel Prize in Physics in 1970. MHD on the other hand is concerned with the study of the magnetic fields interactions and electrically conducting fluids in motion. MHD flows have numerous applications in the industries which includes MHD flow meters, MHD pumps just to mention a few. MHD flow in various physical phenomenon have been carried out by different Scientist. Sharma and Singh [13] studied the effects of variable thermal conductivity and heat source/sink on MHD flow near a stagnation point of a linearly stretching sheet. Kareem et al. [14] studied hydromagnetic reactive fluid flow through horizontal porous plates with radiation and internal heat generation. Salem [15] investigated the effects of variable viscosity and thermal conductivity on MHD flow and heat transfer in viscoelastic fluid over a stretching sheet. Shanker and Kishan [16] discussed the effect of mass transfer on the MHD flow past an impulsively started vertical plate with variable temperature or constant heat flux. Molla, et al [17] examined MHD natural convection flow of an isothermal sphere with temperature dependent viscosity effect. Hazarika et al [18] investigated MHD flow past a vertical plate with the effects of variable viscosity and thermal conductivity. MHD flow of nonlinear radiative heat and mass transfer over a stretching surface with variable conductivity and viscosity was examined by Okedoye et al [20] . Salawu and Amoo [21] discussed MHD Flow in a Porous Medium with the effects of Variable Viscosity and Thermal Conductivity on Dissipative Heat and Mass Transfer of the flow. Makinde and Aziz [22] have investigated flow through porous medium that MHD effects are present. Hunegnaw and Naikoti [19] examined MHD effects on heat transfer over stretching sheet embedded in porous medium with variable viscosity, viscous dissipation.

The Darcy–Forchheimer model is the most widely used Darcian flow modification when it comes to similarity inertia effects. It takes into account both the viscous and the inertia acting on the fluid as well as the forces exerted by the magnetic field. Falana et al [26] examined the Similarity Solution of Heat and Mass Transfer Flow of a Nanofluid across a Porous Plate in a Darcy-Forchheimer Flow. Seddeek [27] examined the impacts of thermophoresis and viscous dissipation in Darcy–Forchheimer mixed convection flow suturing porous medium. Shehzad et al [28] investigated Darcy–Forchheimer flow of variable thermal conductivity Oldroyd-B liquid with linear convection and heat flow through Cattaneo-Christov theory past a vertical sheet. Hayat et al [29] analyzed Maxwell fluid through temperature dependent thermal conductivity and heat flux of Darcy–Forchheimer flow through Cattaneo-Christov theory.

To further gain more understanding on the study of MHD flow, this paper examined MHD Darcy-Forchheimer Slip Flow in a Porous Medium with Variable Thermo-Physical Properties. In the present research, we investigate slip flow of an electrically conducting fluid in a porous media with variable Thermo-Physical Properties (variable viscosity and thermal conductivity). The influence of various physical parameters on the behavior of velocity and temperature profile of the fluid are discussed in details.

II. PROBLEM FORMULATION

Consider a two-dimensional steady laminar boundary layer flow of an incompressible fluid. A magnetic field of strength B_0 is applied in the direction of y-axis as shown in Fig. 1. Temperature and concentration at the surface of the sheet are denoted by T_w and C_w whereas ambient temperature and concentration are indicated by T_∞ and C_∞ where $T_w > T_\infty$ moreover, fluid concentration is $C_w > C_\infty$. The porous layer is homogeneous and isotropic. Furthermore, the effects exponential temperature-dependent heat source/sink, and variable thermal and molecular diffusivity are also considered during mathematical formulation of the problem. The flow is characterized by temperature dependent viscosity and conductivity. Taking into considerations the above assumptions with the boundary layer approximations, the full equation of motion for a two-dimensional flow in Cartesian form regarding continuity, momentum, energy, and concentration are given

$$\frac{\partial u}{\partial x}+\frac{\partial v}{\partial y}=0 \tag{1}$$

$$u\frac{\partial u}{\partial x}+v\frac{\partial u}{\partial y}=\frac{1}{\rho}\frac{\partial P}{\partial x}+\frac{1}{\rho}\frac{\partial}{\partial y}\left(\mu_T\frac{\partial u}{\partial y}\right)-\frac{\sigma B_0^2 u}{\rho}\mp g\left(\frac{\nu}{K_1}\right)|\hat{u}|u +g\left(\beta_\tau(T-T_\infty)+\beta_c(C-C_\infty)\right) \tag{2}$$

$$\rho c_p\left(u\frac{\partial T}{\partial x}+v\frac{\partial T}{\partial y}\right)=\frac{\partial}{\partial y}\left(k_T\frac{\partial u}{\partial y}\right)+\mu\left(\frac{\partial u}{\partial y}\right)^2-\sigma B_0^2u^2 -\left(\frac{\kappa u_w(x)}{x\nu}\right)\left[\frac{A^*(T_w-T_\infty)}{bx}(u-U)+B^*(T-T_\infty)\right] \tag{3}$$

$$\rho\left(u\frac{\partial C}{\partial x}+v\frac{\partial C}{\partial y}\right)=D\frac{\partial^2 C}{\partial y^2}+A(C-C_\infty)+D_T\frac{\partial^2 T}{\partial y^2}-\frac{\partial}{\partial y}(V_T C) \tag{4}$$

Following Arunachalam and Rajappa [30] and Chaim [6] the thermal conductivity K_T is taken as

$$K_T=k\frac{T}{T_\infty}, \tag{5}$$

By Hafiz et al. [31], temperature dependent viscosity is defined as

$$\mu_T=\mu\big(a+b_1(T_\infty-T)\big), \tag{6}$$

The velocity of thermophoretic force V_T is defined similar to Chu et al. []

$$V_T=\frac{k^*\nu}{T_\infty}\left(\frac{\partial T}{\partial y}\right), \tag{7}$$

In the above system of equations each of term have their usual meaning.

Following similar boundary conditions used by Aziz et al. [32], the appropriate partial slip boundary conditions for the velocity, temperature and concentration boundary conditions are given by:

$$u=L_1\left(\frac{\partial u}{\partial y}\right), v=v_w, T=T_w+D_1\left(\frac{\partial T}{\partial y}\right), C=C_w+N_1\left(\frac{\partial C}{\partial y}\right)\ at\ y=0, \quad u\to U_\infty, T\to T_\infty, C\to C_\infty\ as\ y\to\infty \tag{8}$$

In equations (8) $L_1=L(Re_x)^{1/2}$ (velocity slip factor), $D_1=D(Re_x)^{1/2}$ (thermal slip factor) and $N_1=N_0(Re_x)^{1/2}$ (mass slip factor). Here L, D and N_0 are the initial values of velocity, thermal and mass slip factors respectively and all have dimension of length. The $Re_x=\frac{U_\infty x}{\nu}$ is the local Reynolds number. The velocity v_w defines suction or blowing through the porous medium and is written as $v_w=v_0/\sqrt{x}$. In this relation is constant linked with suction if $v_0<0$ and blowing when $v_0>0$.

In the free stream,

$$u \to U_\infty(t) = , T \to T_\infty, C \to C_\infty \tag{9}$$

Thus, by equation (8), (2) gives

$$-\frac{1}{\rho}\frac{\partial P}{\partial x} = U_\infty \frac{\partial U_\infty}{\partial x} + \frac{\sigma B_0^2 U_\infty}{\rho} \pm g\left(\frac{\nu}{K_1}\right)|\hat{u}|U_\infty \tag{10}$$

Using equations (5), (6) and (9) in equations (2) and (3), we obtain the full governing equation of the motion for MHD Darcy Forchheimer slip flow in a porous medium with variable thermo-physical properties as stated below:

$$\begin{aligned} u\frac{\partial u}{\partial x} + v\frac{\partial u}{\partial y} = U_\infty \frac{\partial U_\infty}{\partial x} + \frac{1}{\rho}\frac{\partial}{\partial y}\Big(\mu\big(a + b_1(T_\infty - T)\big)\frac{\partial u}{\partial y}\Big) - \frac{\sigma B_0^2}{\rho}(u - U_\infty) \\ \mp g\left(\frac{\nu}{K_1}\right)|\hat{u}|(u - U) + g\big(\beta_\tau(T - T_\infty) + \beta_c(C - C_\infty)\big) \end{aligned} \tag{11}$$

$$\begin{aligned} \rho c_p\left(u\frac{\partial T}{\partial x} + v\frac{\partial T}{\partial y}\right) = \frac{\partial}{\partial y}\left(k\frac{T}{T_\infty}\frac{\partial T}{\partial y}\right) + \mu\left(\frac{\partial u}{\partial y}\right)^2 - \sigma B_0^2 u^2 \\ -\left(\frac{\kappa u_w(x)}{x\nu}\right)\left[\frac{A^*(T_w - T_\infty)}{bx}(u - U) + B^*(T - T_\infty)\right] \end{aligned} \tag{12}$$

$$\rho\left(u\frac{\partial C}{\partial x} + v\frac{\partial C}{\partial y}\right) = D\frac{\partial^2 C}{\partial y^2} + A(C - C_\infty) + D_T\frac{\partial^2 T}{\partial y^2} - \frac{\partial}{\partial y}(V_T C) \tag{13}$$

III. METHOD OF SOLUTION

A. Similarity Transformation

To solve the system of equations (11)–(13) along with the related boundary conditions (8) similarity technique is used. We adopt a similarity transformations similar to the one used by Bhattacharyya et al. [33] and Aziz et al. [32]:

$$\psi = \sqrt{U_\infty \nu x} f(\eta),\ \ \theta(\eta) = \frac{T - T_\infty}{T_w - T_\infty}, \phi(\eta) = \frac{C - C_\infty}{C_w - C_\infty} \tag{14}$$

where η is similarity variable and it is given as $\eta = \sqrt{Re_x}(y/x)$.

Introducing the above transformations in equations (1)–(4), we obtain the self-similar system of ordinary differential equations thus we have

$$\begin{aligned} \frac{\partial}{\partial \eta}\left(\big(1 - \lambda\theta(\eta)\big)\frac{\partial^2 f(\eta)}{\partial \eta^2}\right) + \frac{1}{2} f(\eta)\frac{\partial^2 f(\eta)}{\partial \eta^2} - Ha\left(\frac{\partial f(\eta)}{\partial \eta} - 1\right) \\ \mp Fs\left(\frac{\partial f(\eta)}{\partial \eta} - 1\right) + Gr\big(N\,\theta(\eta) + \phi(\eta)\big) + 1 = 0 \end{aligned} \tag{15}$$

$$\begin{aligned} \frac{\partial}{\partial \eta}\left(\big(1 + \alpha\theta(\eta)\big)\frac{\partial\,\theta(\eta)}{\partial \eta}\right) + \frac{Pr}{2} f(\eta)\frac{\partial\,\theta(\eta)}{\partial \eta} + Ec\big(1 - \lambda\theta(\eta)\big)\left(\frac{\partial^2 f(\eta)}{\partial \eta^2}\right)^2 \\ -EcHa\left(\frac{\partial f(\eta)}{\partial \eta}\right)^2 - \boldsymbol{\alpha_2}[\alpha_1(f'(\eta) - 1) + \theta(\eta)] = 0 \end{aligned} \tag{16}$$

$$\frac{\partial^2 \phi(\eta)}{\partial \eta^2} + \frac{Sc}{2} f(\eta)\frac{\partial \phi(\eta)}{\partial \eta} + \gamma\phi(\eta) + Sr\frac{\partial^2\,\theta(\eta)}{\partial \eta^2} - \delta\frac{\partial}{\partial \eta}\left(\frac{\partial\,\theta(\eta)}{\partial \eta}\phi(\eta)\right) = 0 \tag{17}$$

Invoking on equation (8), the fact that

$$L_1 = L(Re_x)^{1/2}, D_1 = D(Re_x)^{1/2}, N_1 = N_0(Re_x)^{1/2}, v_w = v_0/\sqrt{x}, Re_x = \frac{U_\infty x}{\nu} \tag{18}$$

The self-similar boundary conditions become

$$\begin{aligned} f'(0) = \tau_1\frac{\partial f'(\eta)}{\partial \eta}, f(0) = \pm S, \theta(0) = 1 + \tau_2\frac{\partial\,\theta(0)}{\partial \eta}, \phi(\eta) = 1 + \tau_3\frac{\partial \phi(0)}{\partial \eta} \\ f'(\eta) \to 1, \theta(\eta) \to 0, \qquad \phi(\eta) \to 0\ as\ \eta\ \to \infty \end{aligned} \tag{19}$$

Where $S > 0$ i.e $(v_0 < 0)$ corresponds to suction and $S < 0$ i.e $(v_0 > 0)$ corresponds to blowing, τ_1 is the velocity slip parameter, τ_2 is the thermal slip parameter and τ_3 is a mass slip parameter.

B. Rate of Flow at the wall

Some engineering parameters of curiosity in the flow are shear strees at the wall c_f, Nusselt number Nu_x and local Sherwood number Sh_x defined respectively as;

$$C_f = \frac{\tau_w}{\rho u_w v_w}, \tau_w = \mu \left.\frac{\partial u}{\partial y}\right|_{y=0}, Nu_x = \frac{E_a q_w}{k R_g T_\infty^2}, q_w = -k \left.\frac{\partial T}{\partial y}\right|_{y=0},$$

$$Sh_x = \frac{J_w}{D(C_w - C_\infty)}, J_w = -D \left.\frac{\partial C}{\partial y}\right|_{y=0}$$

Using similarity transformation, we have

$$\begin{aligned} \tau &= C_f \sqrt{\frac{x}{\nu U_\infty}} = \left(1 - \lambda\theta(\eta)\right) \left.\frac{\partial^2 f(\eta)}{\partial \eta^2}\right|_{\eta=0}, \\ Nu &= Nu_x \sqrt{\frac{U_\infty}{\nu x}} = -\left(1 + \alpha\theta(\eta)\right) \left.\frac{\partial \theta(\eta)}{\partial \eta}\right|_{\eta=0}, \\ Sh &= Sh_x \sqrt{\frac{U_\infty}{\nu x}} = -\left.\frac{\partial \phi(\eta)}{\partial \eta}\right|_{\eta=0}. \end{aligned} \tag{20}$$

Where the emerging governing parameter are

$$\begin{aligned} &Sr = \frac{D_T(T_w - T_\infty)}{D(C_w - C_\infty)}, \gamma = \frac{\nu A x}{D U_\infty}, \delta = \frac{k^* \nu (T_w - T_\infty)}{D T_\infty}, Grc = g \frac{x}{U_\infty^2} \beta_c (C_w - C_\infty), N = \frac{\beta_\tau (T_w - T_\infty)}{\beta_c (C_w - C_\infty)}, N_0 \frac{U_\infty}{\nu} = \tau_3, \\ &Ec = \frac{\mu}{k} \frac{U_\infty^2}{(T_w - T_\infty)}, \alpha_1 = \frac{A^* U_\infty}{b x B^* (T_w - T_\infty)}, \alpha = \frac{(T_w - T_\infty)}{T_\infty}, Ha = \frac{\sigma B_0^2}{\rho} \frac{x}{U_\infty}, \alpha_2 = B^* \left(\frac{u_w(x)}{U_\infty}\right), Pr = \frac{\rho c_p}{k}, \\ &Grt = \frac{xg}{U_\infty^2} \beta_\tau (T_w - T_\infty), Fs = g \frac{x}{U_\infty} \left(\frac{\nu}{K_1}\right) |\hat{u}|, \lambda = \frac{b}{a}(T_w - T_\infty), S = -2 \frac{v_0}{\sqrt{U_\infty \nu}}, L \frac{U_\infty}{\nu} = \tau_1, D \frac{U_\infty}{\nu} = \tau_2, S_c = \frac{\mu}{D}, \end{aligned} \tag{21}$$

IV. RESULTS AND DISCUSSIONS

The numerical computations are performed for several values of dimensionless parameters like Darcy-Forchheimer parameter, t*hermal Grashof number*, Eckert number, Prandtl number and Schmidt number on the dimensionless velocity, temperature and mass transfer. The skin friction and heat transfer rates from a porous medium with slip flow are investigated numerically and presented as follows. For the verification of the accuracy of the applied numerical method, at first, we compare our results corresponding to the velocity and shear stress profile for $Fs = \tau_1 = 0$ (slip at the boundary) with the available results of Aziz [34] and Makinde [22] as presented in Table 1 and found them to be in agreement.

Table 1: Computations showing comparison with Aziz (2009)[34] and Makinde (2010)[22]

Bi	$\theta(0)$	$-\theta'(0)$	$\theta(0)$	$-\theta'(0)$	$\theta(0)$	$-\theta'(0)$
	Aziz (2009)		**Makinde 2010**		**Present**	
0.05	0.1447	0.0428	0.14466	0.04276	0.14466116	0.04276694
0.10	0.2528	0.0747	0.25275	0.07472	0.25275805	0.07472420
0.20	0.4035	0.1193	0.40352	0.11929	0.40352253	0.11929549
0.40	0.5750	0.1700	0.57501	0.16999	0.57501397	0.16999441
0.60	0.6699	0.1981	0.66991	0.19805	0.66991555	0.19805067
0.80	0.7302	0.2159	0.73016	0.21586	0.73016999	0.21586401
1.00	0.7718	0.2282	0.77182	0.22817	0.77182215	0.22817785
5.00	0.9441	0.2791	0.94417	0.27913	0.94417378	0.27913108
10.00	0.9713	0.2871	0.97128	0.28714	0.97128538	0.28714622
20.00	0.9854	0.2913	0.98543	0.29132	0.98543355	0.29132892

Table 2: Effect of variation of Fs, Ha, Grt, and Grc on $f'(0), f''(0), \phi(0), \phi'(0), \theta(0), \theta'(0)$.

	$f'(0)$	$f''(0)$	$\phi(0)$	$\theta(0)$	$\theta'(0)$	τ	Nu	Sh
Fs =0.0	0.1873	1.2487	0.9973	0.7000	-0.0300	0.8991	0.0237	0.0269
Fs =0.2	0.1826	1.2172	0.9963	0.6990	-0.0301	0.8768	0.0238	0.0373
Fs =0.4	0.1788	1.1923	0.9949	0.6967	-0.0303	0.8600	0.0240	0.5144
Fs =0.6	0.1770	1.1799	0.9929	0.6923	-0.0308	0.8532	0.0244	0.7109
Ha =0.0	0.1827	1.2181	0.9958	0.7080	-0.0292	0.8731	0.0230	0.0420
Ha =0.5	0.1871	1.2476	1.0053	0.4931	-0.0507	1.0015	0.0432	-0.0526
Ha =1.0	0.1969	1.3128	1.0124	0.2800	-0.0720	1.1658	0.0660	-0.1237
Ha =3.5	0.2357	1.5714	1.0405	-0.7878	-0.1788	2.0666	0.2210	-0.4048
Grt =0.0	0.0815	0.5434	1.0363	0.9822	-0.0018	0.3299	0.0013	-0.3626
Grt =0.2	0.1391	0.9273	1.0074	0.7821	-0.0218	0.6372	0.0167	-0.0737
Grt =0.4	0.1825	1.2169	0.9962	0.6994	-0.0301	0.8765	0.0238	0.3759
Grt =0.8	0.2577	1.7182	0.9824	0.6497	-0.0350	1.2717	0.0282	0.1760
Grc =0.0	0.1714	1.1425	0.9963	0.7049	-0.0295	0.8204	0.0233	0.0367
Grc =2.0	0.2725	1.8163	0.9924	0.6780	-0.0322	1.3237	0.0257	0.0758
Grc =4.0	0.3630	2.4198	0.9870	0.7038	-0.0296	1.7386	0.0234	0.1299
Grc =6.0	0.4721	3.1474	0.9795	0.7870	-0.0213	2.1566	0.0163	0.2048

Table 3: Effect of variation of Sr, Ec and S on $f'(0), f''(0), \phi(0), \phi'(0), \theta(0), \theta'(0)$.

	$f'(0)$	$f''(0)$	$\phi(0)$	$\theta(0)$	$\theta'(0)$	τ	Nu	Sh
Sr =0.0	0.1749	1.1659	0.9992	0.7147	-0.0285	0.8326	0.0224	0.0081
Sr =0.5	0.1902	1.2680	0.9929	0.6868	-0.0313	0.9196	0.0249	0.0706
Sr =1.2	0.2055	1.3700	0.9852	0.6697	-0.0330	1.0030	0.0264	0.1481
Sr =2.4	0.2366	1.5775	0.9644	0.6619	-0.3382	1.1599	0.2710	0.3562
Ec =0.0	0.1668	1.1118	1.0027	0.4216	-0.0578	0.9243	0.0505	-0.0266
Ec =0.8	0.1825	1.2169	0.9962	0.6994	-0.0301	0.8765	0.0238	0.0376
Ec =1.8	0.2081	1.3874	0.9856	1.1352	0.0135	0.7574	-0.0089	0.1444
Ec =2.8	0.2435	1.6236	0.9705	1.7106	0.0711	0.5127	-0.0346	0.2950
S =-2.0	0.1016	0.6772	1.0118	0.9769	-0.0023	0.4126	0.0016	-0.1183
S =-2.0	0.1451	0.9672	1.0114	0.8193	-0.0181	0.6502	0.0136	-0.1141
S =2.0	0.2019	1.3459	0.9775	0.6408	-0.0359	1.0009	0.0290	0.2249
S =4.0	0.2852	1.9010	0.8959	0.4375	-0.0563	1.5683	0.0489	1.0408

Table 4: Numerical outcomes of variation of $\alpha, \lambda, \delta, \gamma, \alpha_1$ and α_2 on the wall physical properties{ $f'(0), f''(0), \theta(0), \theta'(0), \phi(0), \phi'(0)$}.

	$f'(0)$	$f''(0)$	$\phi(0)$	$\theta(0)$	$\theta'(0)$	τ	Nu	Sh
α =0.0	0.1838	1.2255	0.9958	0.7172	-0.0283	0.8740	0.0283	0.0417
α =1.0	0.1791	1.1942	0.9975	0.6485	-0.0352	0.8844	0.0579	0.0250
α =2.5	0.1757	1.1713	0.9988	0.5943	-0.4057	0.8929	1.0084	0.1165
α =5.0	0.1729	1.1524	1.0000	0.5462	-0.0454	0.9006	0.1693	0.0000
λ =1.2	0.2789	1.8593	0.9931	0.4443	-0.0556	0.8681	0.0482	0.0688
λ =0.5	0.2164	1.4426	0.9947	0.5933	-0.0407	1.0147	0.0334	0.0534
λ =-0.5	0.1410	0.9401	0.9998	0.8677	-0.0132	1.3479	0.0098	0.2494
λ =-1,2	0.1086	0.7238	1.0052	1.0446	0.0045	1.6312	-0.0031	-0.5230
δ =-1.8	0.2334	1.5558	0.9576	0.6539	-0.0346	1.1489	0.0278	0.4241
δ =-1.0	0.2010	1.3398	0.9860	0.6713	-0.0329	0.9800	0.0263	0.1397
δ =-0.5	0.1853	1.2353	0.9950	0.6943	-0.0306	0.8922	0.0242	0.0502
δ =0.0	0.1727	1.1513	1.0000	0.7197	-0.0280	0.8198	0.0220	0.0000
γ =-15.0	0.0951	0.6341	0.7577	0.9529	-0.0047	0.3924	0.0034	2.4226
γ =-2.0	0.1170	0.7802	0.8843	0.8817	-0.0118	0.5051	0.0087	1.1570
γ =2.0	0.0790	0.5267	0.9479	1.1504	0.0150	0.2843	-0.0098	0.5213
γ =8.0	0.0815	0.5435	0.9578	1.0338	0.0034	0.3188	-0.0023	0.4220
α_1 =-2.5	0.1125	0.7498	1.0234	-0.5829	-0.1583	0.9246	0.1860	-0.2342
α_1 =-1.5	0.1436	0.9576	1.0116	-0.0850	-0.1009	0.9902	0.1034	-0.1159

α_1 =1.8	0.1825	1.2169	0.9962	0.6994	-0.0301	0.8765	0.0238	0.0376
α_1 =4.8	0.2003	1.3355	0.9876	0.9871	-0.0013	0.8082	0.0009	0.1238
α_2 =0	0.2036	1.3571	0.9870	1.0759	0.7590	0.7731	-0.5140	0.1303
α_2 =1	0.1825	1.2169	0.9962	0.6994	-0.0301	0.8765	0.0238	0.0376
α_2 =2	0.1728	1.1522	1.0004	0.5242	-0.0476	0.9106	0.0401	-0.3640
α_2 =4	0.1635	1.0898	1.0042	0.3552	-0.0645	0.9350	0.0576	-0.4193

Figures 2-12 depicts the nature of velocity profile over the variations of Darcy-Forchheimer parameter Fs, Hartmann number Ha, thermal Grashof number Grt, mass Grashof number Grc, temperature dependent viscosity λ, thermophoresis factor δ, Suction S, Soret number S_r , Eckert number Ec , non-uniform heat source/sink α_1 and velocity slip parameter τ_1 respectively. Figure 2 clearly indicate that the velocity of the fluid increases with increase in the Darcy-Forchheimer term. The variation in it reduces the fluid kinetic viscosity as a result the flow speed increases. Hartman number decreases the flow velocity, this is because it represents magnetic force which induce Lorentz force into the flow as seen in Figure 3. The thermal and mass Grashof number increases the fluid velocity as reported in Figures 4 and 5. With increasing values of the temperature dependent viscosity, the fluid velocity increases as seen in Figure 6. As observed in Figure 7 is the analysis of

Table 5: Effect of variation of τ_1, τ_2, τ_3, Pr *and* Sc on $f'(0), f''(0), \phi(0), \phi'(0), \theta(0), \theta'(0)$.

	$f'(0)$	$f''(0)$	$\phi(0)$	$\theta(0)$	$\theta'(0)$	τ	Nu	Sh
τ_1 =0.1	0.1272	1.2722	0.9961	0.7641	-0.0236	0.8834	0.0182	0.0389
τ_1 =0.5	0.4685	0.9369	0.9962	0.3832	-0.0617	0.7933	0.0546	0.0385
τ_1 =1.0	0.7083	0.7083	0.9951	0.1454	-0.0855	0.6671	0.0817	0.0489
τ_1 =1.5	0.8560	0.5707	0.9942	0.0117	-0.0988	0.5680	0.0985	0.0579
τ_2 =0.0	0.1808	1.2054	0.9946	0.6734	0.0000	0.8807	0.0000	0.0537
τ_2 =1.0	0.1913	1.2753	1.0041	0.8250	-0.1750	0.8544	0.1317	-0.0406
τ_2 =3.0	0.1973	1.3150	1.0091	0.9099	-0.2703	0.8364	0.1965	-0.0912
τ_2 =5.0	0.1994	1.3292	1.0109	0.9394	-0.3031	0.8297	0.2177	-0.1085
τ_3 =0.0	0.1829	1.2191	1.0000	0.6987	-0.0301	0.8784	0.0238	0.0380
τ_3 =0.5	0.1815	1.2101	0.9825	0.7007	-0.0299	0.8709	0.0236	0.3505
τ_3 =1.5	0.1794	1.1962	0.9549	0.7036	-0.0296	0.8595	0.0234	0.0301
τ_3 =2.5	0.1779	1.1861	0.9344	0.7056	-0.0294	0.8513	0.0232	0.2625
Pr =0.01	0.1859	1.2391	0.9952	0.7636	-0.2364	0.8606	0.1822	0.0477
Pr =0.30	0.1856	1.2375	0.9952	0.7609	-0.0239	0.8608	0.0185	0.0477
Pr =0.72	0.1825	1.2169	0.9962	0.6994	-0.0301	0.8765	0.0238	0.0376
Pr =4.00	0.1740	1.1600	1.0002	0.5244	-0.0476	0.9167	0.0401	-0.1914
Sc =0.57	0.1848	1.2319	0.9953	0.6925	-0.0308	0.8907	0.0244	0.0473
Sc =0.99	0.1735	1.1567	1.0028	0.7278	-0.0272	0.8200	0.0213	-0.0282
Sc =1.14	0.1710	1.1400	1.0058	0.7363	-0.0264	0.8043	0.0205	-0.0575
Sc =1.50	0.1665	1.1103	1.0130	0.7519	-0.0248	0.7763	0.0192	-0.1301

the theromphoreis parameter, raising this parameter increases the velocity of the fluid. Figure 8 shows the effect of Suction parameter of the velocity profile. Herein S<0 (suction) and S>0 (blowing). In case of suction, it provides impending motion to flow thereby resulting in drop of flow velocity as reported in Figure 8. The reverse is the case for blowing. Figure 9 shows the effect of variation in Soret number on the velocity profile. It is obvious that the velocity improve by increasing the Soret number. Figure 10 shows the influence of Eckert number on the velocity profile. There is an increase in velocity of the fluid with an increase in the Eckert number. Increasing α_1 results to increase in the velocity profile as seen in Figure 11. The variation in velocity design via velocity slip parameter is discussed in Figure 12. It was observed that as velocity slip parameter increases the fluid velocity was oppose thereby reducing the velocity of the fluid.

Figure 13-18 demonstrates the behavior of thermal Grashof number Grt, temperature dependent thermal conductivity (variable thermal conductivity) α, temperature dependent viscosity (variable viscosity) λ, Eckert number Ec, temperature dependent heat source α_2 and thermal slip parameter τ_1 respectively on the temperature profile. Figure 13 show the effect of thermal Grashof number on the temperature. It is observed, the increase in the thermal Grashof number decreases the temperature of the fluid. Figure 14 depicts the behavior of variable thermal conductivity; the temperature increases as a result of increase in the variable thermal conductivity this is so because ... while the temperature decreased when the temperature variable viscosity was increased as seen in Figure 15. The increasing of Eckert number and the thermal slip

parameter effect provides an increase in the fluid temperature as seen in Figures 16 and 18. The temperature decreases as a result of increase in the thermal slip parameter of the temperature profile as seen in Figure 17.

The behavior of the mass transference profile against Hartmann number Ha, thermal Grashof number Grt, temperature dependent viscosity λ, thermophoresis factor δ, Suction S, Soret number S_r and mass slip parameter τ_1 respectively was also investigated.

The effect of Lorentz force in terms of Hartmann number on chemical species is shown in Figure 19. It could be deduced from this figure that increasing the Lorentz force on the flow field brings about increase in the chemical species boundary layers. Specifically, when Hartmann number is increased from 0.0 to 0.5, the chemical species boundary layers increased by 27.4% at point 1.2 units away from the surface of the flow. Further increase of Hartmann number from 0.5 to 1.0 and 1.0 to 1.5 yields 44.7% and 70.7% respectively. Similar effect is observed with temperature dependent viscousity and Soret number influences on Chemical Species as shown in Figures 21 and 24 respectively. When Hartmann number is increased from 0.0 to 0.5, 0.5 to 1.0 and 1.0 to 1.5 in both cases respectively yields 4%, 8%and 6% and, 21.8%, 21.9% and 51% respectively. While Chemical Species boundary layers decline with increase in Thermal Grashof number, δ, suction and concentration slip condition as shown in Figures 20, 22, 23 and 25 respectively. The figures indicate the fact that concentration is higher in the body, close to the surface of the fluid. We also discovered that in all cases, the maximum concentration shift to the right as the governing parameter increases.

The three most important physical component of the problem are the shear stress at the wall, heat transfer and mass transfer rate at the surface. Table 2 show the behaviour of Darcy-Forchheimer parameter F_s, Hartman number H_a, thermal Grashof number Grt and mass Grashof number Grc. The shear stress at the wall was decrease when F_s was increased (from 0.2-0.6) while shear stress decreases for increasing values of $H_a, Grc\ and\ Grt$. The heat transfer rate at the surface was increased when $F_s, H_a, Grc\ and\ Grt$ was increased. The mass transfer rate at the surface increase when $F_s, Grc\ and\ Grt$ was increase and decreases for $H_a$increase. Table 3 list the values of shear stress, heat and mass transfer at the surface as a function of Soret number s_r, Erkect number E_c and Suction S. The shear stress at the wall was increase when $S_r\ and\ S$ was increased while shear stress decreases for increasing values of E_c. The heat transfer rate at the surface was increased when $S_r\ and\ S$ was increased and decreases when E_c was increased. $S_r,\ E_c\ and\ S$ increase resulted to increasing the mass transfer rate at the surface increase. The shear stress at the wall, heat and mass transfer at the surface as a function of $\alpha, \lambda,\ \delta, \gamma, \alpha_1$ and α_2 is shown in Table 4. The shear stress at the wall was increase when $\alpha,\ \delta\ and\ \alpha_2$ was increased while shear stress decreases for increasing values of $\lambda,\ \gamma,$ and $\alpha_{1\ c}$. The heat transfer rate increase when $\alpha, \gamma,$ and $\alpha_2$was increased and decreases when $\lambda,\ \delta\ and\ \alpha_1$ was increased. The mass transfer rate at the surface was decreased when $\alpha, \lambda,\ \delta, \gamma, \alpha_1$ and $\alpha_2$was increased. The shear stress at the wall, heat and mass transfer at the surface as a function $\tau_1, \tau_2, \tau_3,$ Pr $and\ Sc$ is shown in Table 5. The shear stress at the wall was increase when P_r was increased while shear stress decreases for increasing values of $\tau_1, \tau_2, \tau_3\ and\ Sc$. The heat transfer rate at the surface was increased when $\tau_1, and\ \tau_2$ was increased and decreases when $\tau_3,$ Pr $and\ Sc$ is increased. The mass transfer rate at the surface was decreased when $\tau_2, \tau_3,$ Pr $and\ Sc$ was increased and increases only when τ_1 was increased.

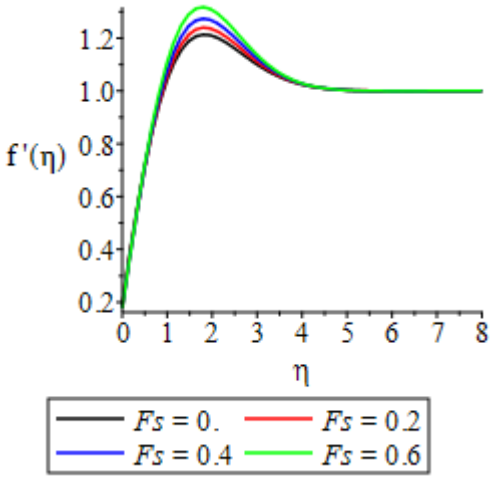

Figure 2: Effect of F_s on the velocity profile

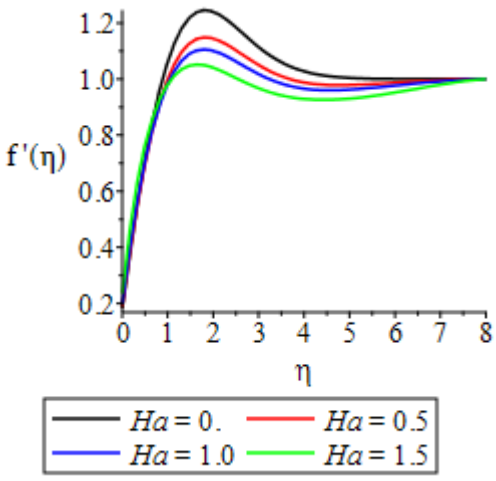

Figure 3: Effect of H_a on the velocity profile

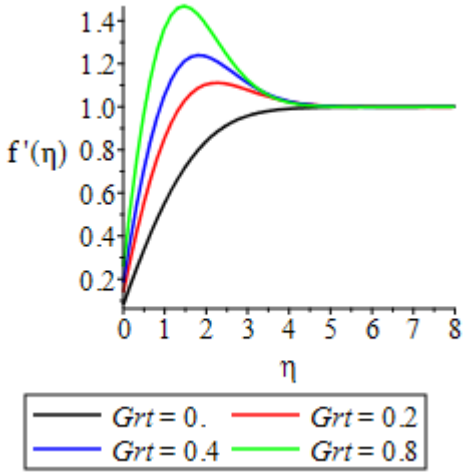

Figure 4: Variation of Grt on the velocity profile

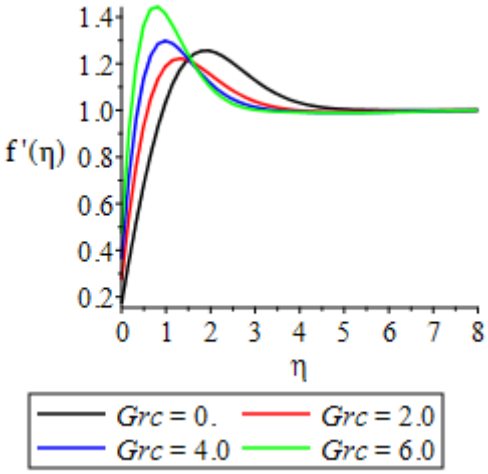

Figure 5: Variation of Grc on the velocity profile

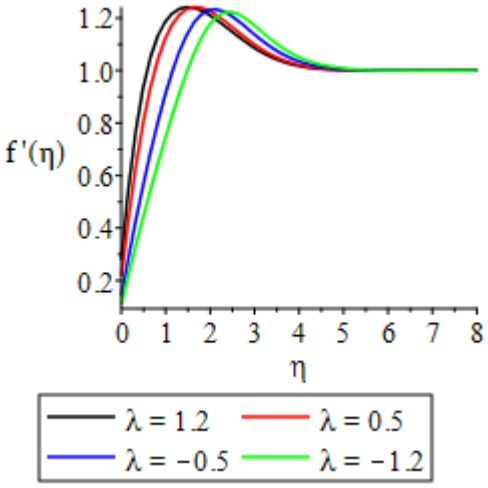

Figure 6: Behaviour of velocity against λ

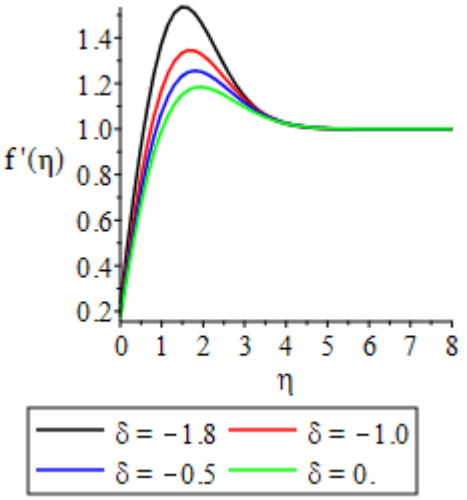

Figure 7: Behaviour of velocity against δ

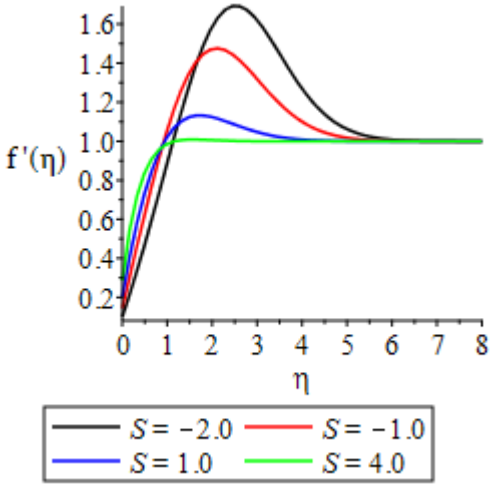

Figure 8: Velocity profile for S variations

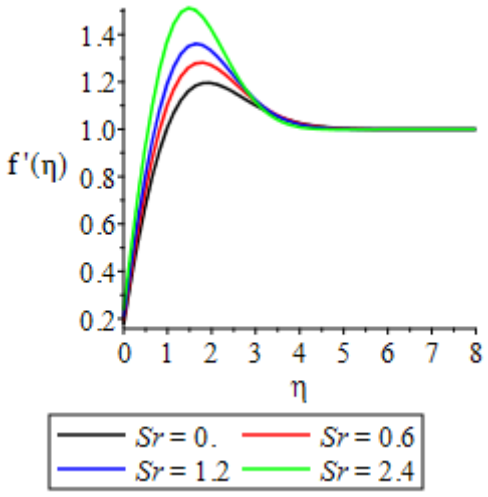

Figure 9: Velocity profile for S_r variations

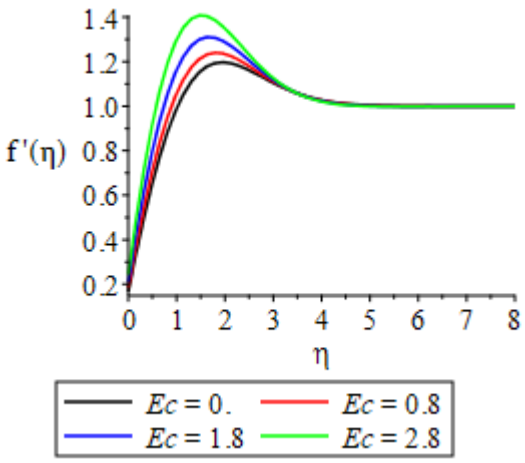

Figure 10: Effect of E_c the velocity profile

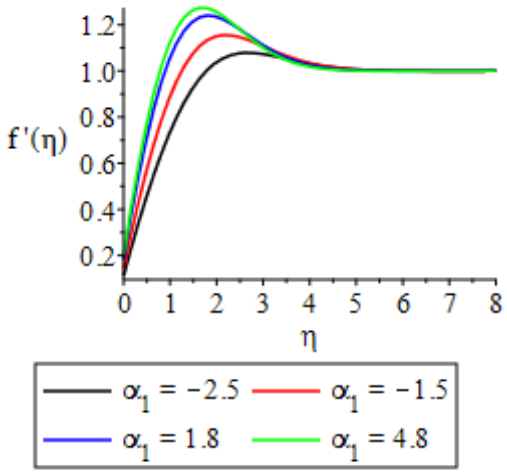

Figure 11: Effect of α_1 the velocity profile

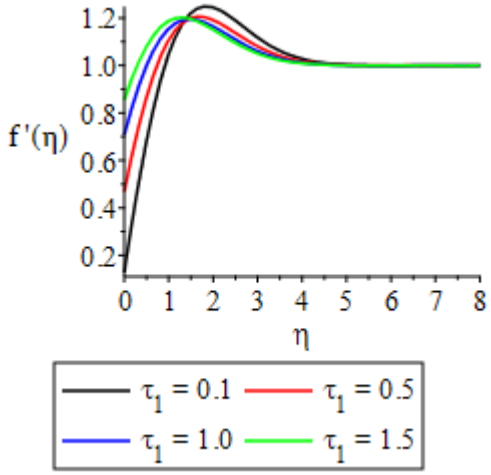

Figure 12: Effect of τ_1 the velocity profile

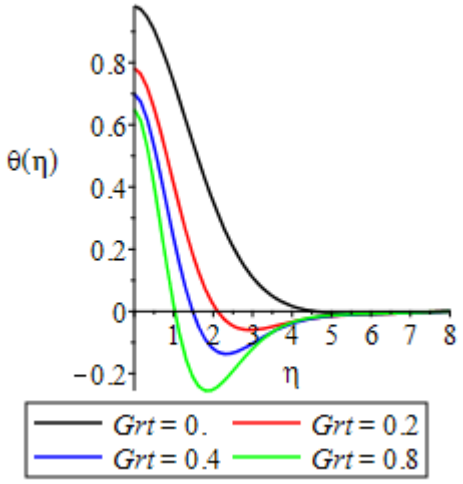

Figure 13:Variation of Grt on the temperature

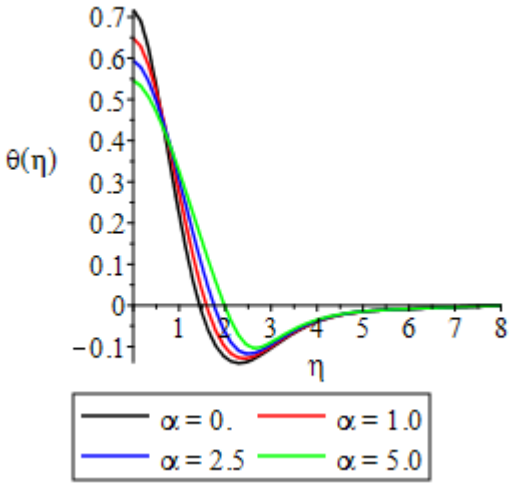

Figure 14: α effect on the temperature profile

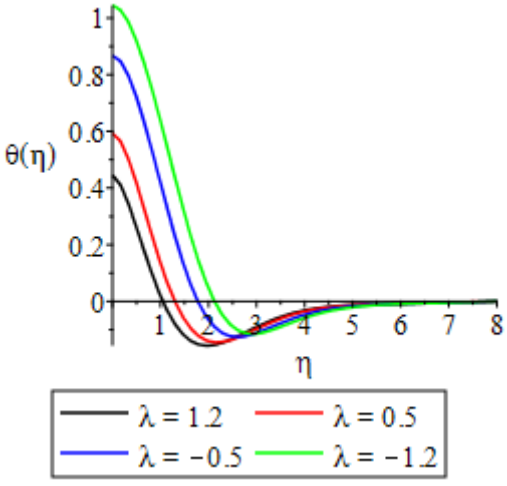

Figure 15: λ effect on the temperature profile

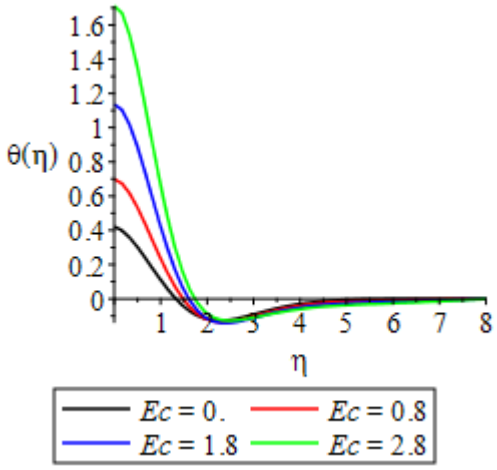

Figure 16: Effect of E_c on the temperature

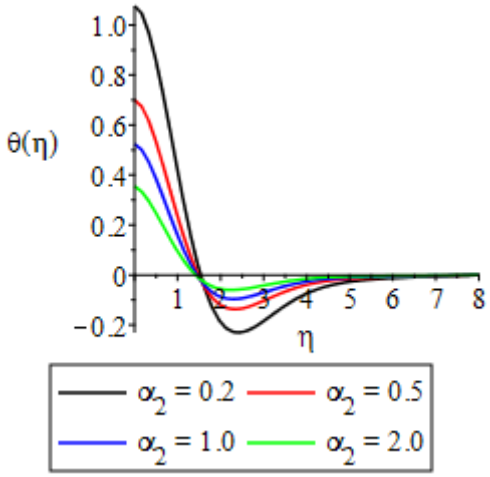

Figure 17: Effect of α_2 on the temperature

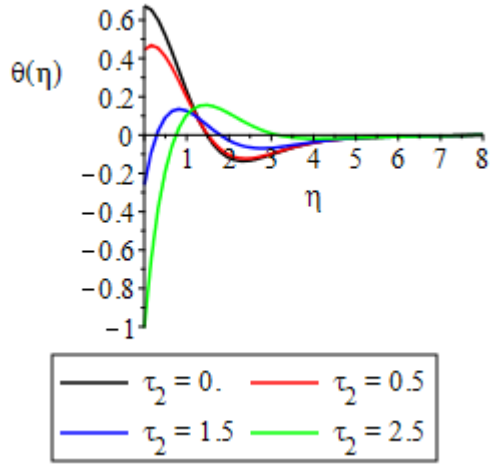

Figure 18: Nature of τ_2 on the temperature

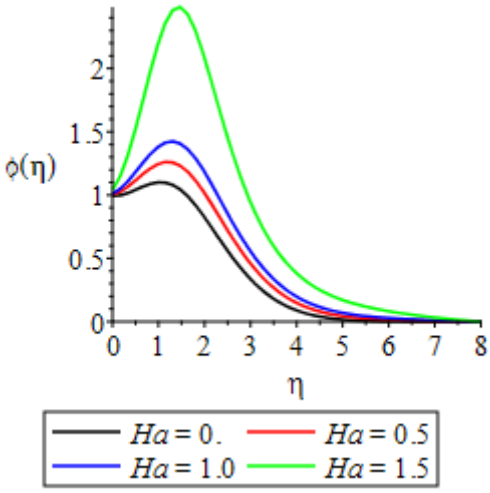

Figure 19: Effect of H_a on the concentration

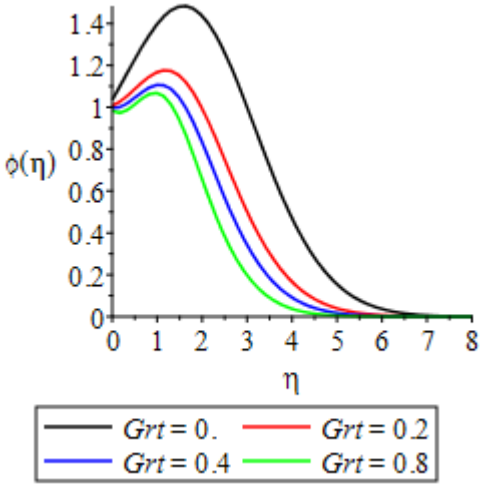

Figure 20: Nature of Grt on the concentration profile

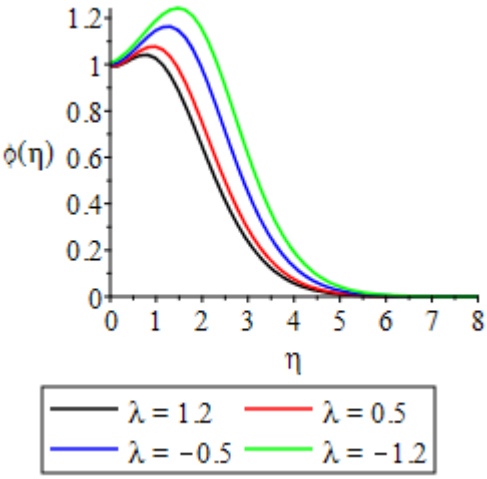

Figure 21: Nature of λ on the concentration profile

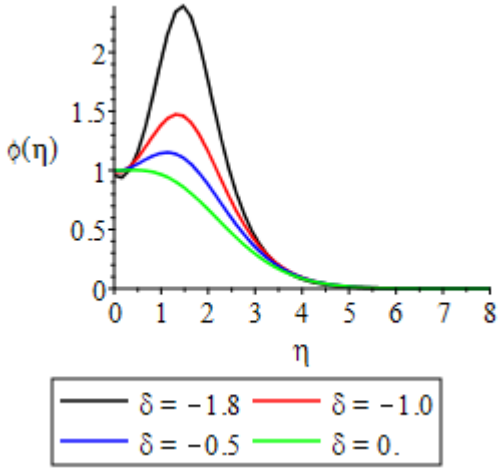

Figure 22: Behaviour of δ on the concentration profile

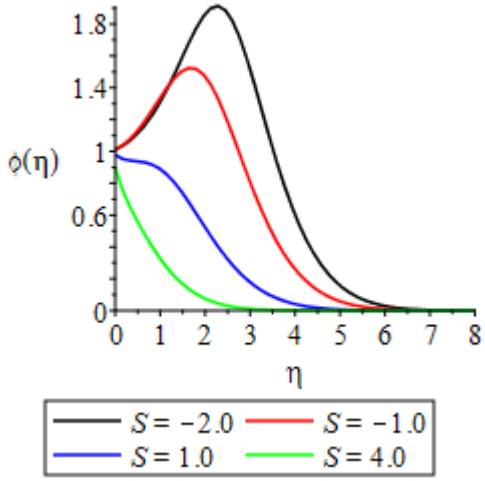

Figure 23: Behaviour of S against concentration profile

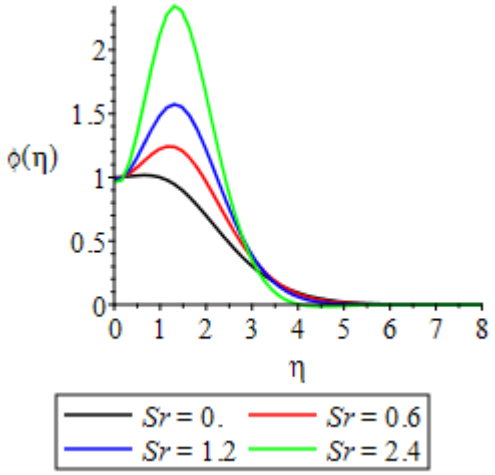

Figure 24: Effect of S_r on the concentration profile

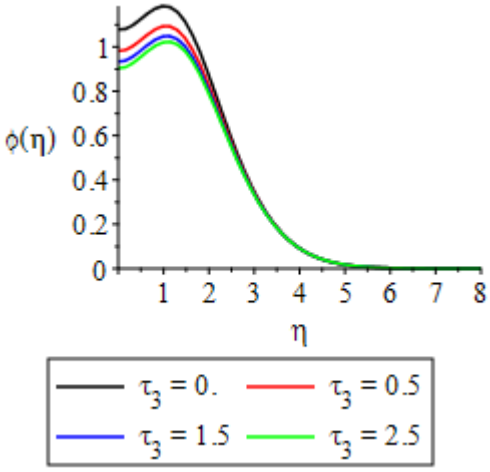

Figure 25: Nature of τ_3 on the concentration profile

V. CONCLUSION

MHD Darcy-Forchheimer Slip Flow in a Porous Medium with Variable Thermo-Physical Properties is presented. The coupled system of ODEs was solved numerically. Observations were based on the Darcy-Forchheimer parameter, velocity slip parameter and suction parameters. Some dimensionless parameters like Schmidt number, Soret number, Hartmann and Eckert number were also investigated. We also shown numerical results of the effects of the local skin friction, Nusselt number and Sherwood number in tables. In the end the following observation were made from the analysis:

- When the Darcy-Forchheimer parameter was increased, the fluid velocity increased.
- Increase in velocity slip parameter result in decrease in velocity profile whereas thermal slip parameter increase resulted in temperature increase and increase in the mass slip parameter decreases the concentration profile.
- Increase in Suction, variable viscosity and thermal conductivity reduces the concentration profile.
- Skin friction decreases for large Darcy-Forchheimer parameter while heat and mass transfer rates increase.

CONTRIBUTION OF AUTHOR: Each author made an equal contribution.

CONFLICT OF INTEREST: According to the authors, there is no conflict of interest.

ACKNOWLEDGEMENTS: The management of Covenant University is appreciated and thanked by the writers for providing conducive environment and research facilities. We also appreciate the unnamed referees' helpful comments, which helped to improve the final product.

REFERENCES

[1] Y. Menni, A. J. Chamakha and A. Azzi, "Nanofluid transport in porous media: a review," *Special Topics & Reviews in Porous Media: An International Journal*, vol. 10, no. 1, pp 49-64, 2019.

[2] P.G. Saffman, On the boundary condition at the surface of a porous medium, *Studies App. Math.* 50 (1971) 93-101.

[3] T. Hayat, Z. Hussain, A. Alsaedi and B. Ahmad, Heterogeneous-homogeneous reactions and melting heat transfer effects in flow with carbon nanotubes, *J. Mol. Liq.* 220 (2016) 200-207.

[4] M.R. Krishnamurthy, B.J. Gireesha, R.S.R. Gorla and B.C. Prasannakumara, Suspended Particle effect on slip flow and melting heat transfer of nanofluid over a stretching sheet embedded in a porous medium in the presence of nonlinear thermal radiation, *J. Nanofluids 5* (2016) 502-510.

[5] Balla, C.S, Alluguvelli Ramesh, and Naikoti Kishan. Effects of variable viscosity and thermal conductivity on MHD boundary layer flow of Nanofluid with thermal radiation. *Journal of Nanofluid.* Vol. 6, pp. 1–12. 2017.

[6] T. C. Chiam, *Acta Mech.* 129, 63 (1998).

[7] A. Y. Ghaly and M. A. Seddeek, *Chaos, Solitons and Fractals* 19, 61 (2004).

[8] Odda, S.N and .A.M. Farhan, Chebyshev finite difference method for the effects of variable viscosity and variable thermal conductivity on heat transfer to a micro-polar fluid from a non-isothermal stretching sheet with suction and blowing, *Chaos Solution Fract*., Vol. 30(4), pp. 851-858. 2006.

[9] Seddeek, M.A. and F.A. Salama, F.A.The effects of temperature dependent viscosity and thermal conductivity on unsteady MHD convective heat transfer past a semi-infinite vertical porous moving plate with variable suction, *Comp. Mater. Sci*., Vol. 40(2), 2007. pp. 186-192.

[10] F. C. Lai and F. A. Kulacki, *Int J. Heat and Mass Transfer* 33, 1028 (1991).

[11] S. Manjunatha and B. J. Gireesha, *Ain Shams Engineering Journal* 7, 505 (2016).

[12] H. Alfven, "On the existence of electromagnetic-hydromagnetic waves," *Arkiv for Matematik, Astronomi och Fysik*, vol. 29, pp. 1–7, 1943

[13] Sharma, P.R and Singh, G. Effect of variable thermal conductivity and heat source/sink on MHD flow near a stagnation point linearly stretching sheet. *J. Applied Fluid Mech*., 2: 13-21; 2009.

[14] Kareem R.A, Salawu S.O and Yubin Yan . Analysis of transient Rivlin-Ericksen fluid and Irreversibility of exothermic reactive hydromagnetic Variable Viscosity. *J. Appl. Comput. Mech*., 6(1), 26- 36. 2020.

[15] Salem, A.M, Variable viscosity and thermal conductivity effects on MHD flow and heat transfer in viscoelastic fluid over a stretching sheet, *Phys. Lett. A*, Vol. 369 (4), pp. 315-322. 2007

[16] Shanker, B and Kishan, N. (1997). *J. Energy, Heat Mass Transfer* 19, 273

[17] Molla, M.M, Saha, S. C and M. A. Hossain (2012), *J. of Appl. Fluid Mech.* 5, 25.

[18] G. C. Hazarika and S. G. Ch. Utpal, *Mat Ensen Univ.* XX, 45 (2012).

[19] Hunegnaw and K. Naikoti, *Ain Shams Eng. J.* 5, 967 (2014).

[20] Okedoye, A. M and Salawu, S.O. (2019). Effect of nonlinear radiative heat and mass transfer on MHD flow over a stretching surface with variable conductivity and viscosity.

[21] Salawu, S.O. & Amoo, S.A.: Effects of Variable Viscosity and Thermal Conductivity on Dissipative Heat and Mass Transfer of Magnetohydrodynamic Flow in a Porous Medium. *Advances in Multidisciplinary Research Journal*. Vol 2, No.2 Pp 111-122. 2016.

[22] O. D. Makinde and A. Aziz: "MHD mixed convection from a vertical plate embedded in a porous medium with a convective boundary condition," *International Journal of Thermal Sciences*, vol. 49, no. 9, pp. 1813–1820. 2010.

[23] Chen, C.H., 2006. Effect of viscous dissipation on heat transfer in a non-Newtonian liquid film over an unsteady stretching sheet. *J. Non-Newtonian Fluid Mech*., 135: 128-135.

[24] Elbashbeshy, E.M., 1998. Heat transfer over a stretching surface with variable surface heat flux. *J. Phys. D. Applied Phys*., 31: 1951-1954.

[25] Elbashbeshy, E.M.A. and M.A.A. Bazid, 2004. Heat transfer over an unsteady stretching surface. Heat Mass Transfer, 41: 1-4

[26] A. Falana and A. A. Alao, *Current Journal of Applied Science and Technology* 34, 1 (2019).

[27] Seddeek M A. Influence of viscous dissipation and thermophoresis on Darcy-Forchheimer mixed convection in a fluid saturated porous media. *J Colloid Interface Sci* 2006; 293:137-42.

[28] Shehzad S A, Abbasi F M, Hayat T, Alsaedi A. Catteneo-Christov heat flux transfer for Darcy-Forchheimer flow of an Oldroyd-B fluid with variable conductivity and non linear convection. *J Mol Lig* 2016; 224:274-8.

[29] Hayat T, Muhammad T, Al-Mezal S, Liao S J. Darcy-Forchheimer flow with variable thermal conductivity and Catteneo-Christov heat flux. *Int. J Numer Methods Heat Fluid Flow* 2016; 26:2355-69.

[30] Arunachalam, M.; Rajappa, N.R. Forced convection in liquid metals with variable thermal conductivity and capacity. *Acta Mech*. 1978, 31, 25–31.

[31] Hafiz Abdul Wahab, Hussan Zeb, Saira Bhatti, Muhammad Gulistan, Seifedine Kadry, and Yunyoung Nam: Numerical Study for the Effects of Temperature Dependent Viscosity Flow of Non-Newtonian Fluid with Double Stratification. *Appl. Sci.* 2020, *10*, 708; doi:10.3390/app10020708. www.mdpi.com/journal/applsci.

[32] Aziz A, Siddique J.I. Aziz T: Steady Boundary Layer Slip Flow along with Heat and Mass Transfer over a Flat Porous Plate Embedded in a Porous Medium. *PLoS ONE* 9(12): 2014. e114544. doi:10.1371/journal.pone.0114544.

[33] Bhattacharyya K, Mukhopadhyay S, Layek GC: *Steady boundary layer slip flow and heat transfer over a flat porous plate embedded in a porous media. Journal of Petroleum Science and Engineering 78: 304. 2011.*

[34] *Aziz* A: A similarity solution for laminar thermal boundary layer flow over a flat plate with convective surface boundary condition. *Communications in Nonlinear Science and Numerical Simulation* 14: 1064. 2009.

APPENDICES - A

Nomenclature:

y	Axis of flow	Dimensionless group	
u, v	*Velocity component along the x and y-axis*	Bi	Convective heat transfer
T	*Temperature field*	θ	Dimensionless temperature
C	*Concentration field*	ϕ	Dimensionless concentration
g	Gravitational acceleration	Grc	*Mass Grashof number*
B_0	*Magnetic field of uniform strength*	Grt	*Thermal Grashof number*
T_w	Surface temperature	N	buoyancy ratio
T_∞	Ambient temperature	δ	Thermophoersis parameter
C_w	Surface concentration	α	Heat generation parameter
C_∞	Ambient concentration	M	*Magnetic parameter*
β_τ	*Volumetric coefficient of thermal expansion*	Nu	*Nusselt number*
β_c	*Volumetric coefficient of mass expansion*	Sh	*Sherwood number*
K_1	Permeability of Porous medium	Ha	*Hartmann number*
V_T	Thermophoretic force velocity	Sr	*Soret number*
D	*Molecular diffusivity*	Ec	*Eckert Number*
D_T	Thermophoretic Diffusion Coefficient	λ	*Temperature dependent viscosity*
U_∞	Ambient velocity	β	*Heat generation parameter*
Q	*Heat source/sink parameter*	δ	Variable thermal conductivity
L_1	*Slip velocity factor*	F_s	Darcy-Forchheimer Parameter
D_1	*Thermal slip factor*	Pr	*Prandtl number*
N_1	*Mass slip factor*	Sc	*Schmidt number*
τ_w	Shear stress at the wall	Subscript	
q_w	Heat flux at the surface		
J_w	Mass flux at the surface		
Greek Symbol		∞	Ambient condition
ρ	Fluid density	w	wall condition
σ	*Electrical conductivity*		
μ	Fluid viscosity	$0 < \epsilon \ll 1$	